Publishing House
AKAPIT

COMPUTER METHODS IN MATERIALS SCIENCE

Informatyka w Technologii Materiałów

Vol. 9, 2009, No. 1

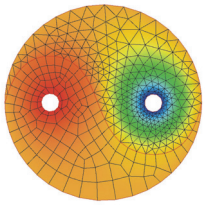

FAILURE MODELLING OF FRICTION STIR WELDED JOINTS IN TENSILE TESTS

GUIDO BORINO[1], LIVAN FRATINI[2], FRANCESCO PARRINELLO[1], ANTONINO BULGARELLA[2]

[1]University of Palermo, Dipartimento di Ingegneria Strutturale e Geotecnica, Palermo, Italy,
[2]University of Palermo, Dipartimento di Tecnologia Meccanica, Produzione ed Ingegneria Gestionale, Palermo, Italy
Corresponding Author: borino@unipa.it (G. Borino)

Abstract

The paper concerns with the mechanical modelling and the finite element simulation of the fracture failure in mode I of linear joints of aluminum friction stir weldings. The problem is analyzed employing a bulk finite strain-hardening plasticity model able to characterize the spatial diffuse plastic strains that initially develop in the neighbouring extended zones of the welding line. Moreover, the decohesion process is described by a zero thickness interface model which is spatially inserted along the line of the welding.

Key words: friction stir welding, finite elements, cohesive interface, failure analysis

1. INTRODUCTION

Friction Stir Welding (FSW) is a solid state welding process in which a specially designed rotating pin is first inserted into the adjoining edges of the sheets to be welded with a proper tilt angle and then moved all along the joint. The tool action produces frictional and plastic deformation heating in the welding zone; actually no melting of material is observed during the process. Recent studies [1] proved that the FSW technique is a relevant alternative to traditional fusion-based welding and gives as a result effective and sound joints even with traditionally difficult to be welded materials.

During the process, the tool rotation speed (R) and feed rate (Vf), determining the specific thermal contribution conferred to the joint, are combined in a way that an asymmetric metal flow is obtained. In particular, an advancing side and a retreating side are observed: the former being characterized by the "positive" combination of the tool feed rate and of the peripheral tool velocity while the latter having velocity vectors of feed and rotation opposite to each other. A detailed observation of the material microstructure [2] highlighted the presence of an area located at the core of the welding, called "nugget", where the original grain and subgrain boundaries appear to be replaced with fine, equiaxed recrystallized grains characterized by a nominal dimension of a few μm. Furthermore, moving from the welding line towards the parent material of the blanks a thermo-mechanically affected zone (TMAZ) is found out, where the stirring action caused by the tool pin determines a distortion of the material grains. Then two layers - Heat affected zones (HAZ) – are seen.

The effectiveness of the obtained joint is strongly dependent on several operating parameters [3]. First of all, the geometric characteristics of the tool which determine both the most relevant part of

 ISSN 1641-8581

the heat flux generated during the process and what is more create the stirring action and then the material flow. Then either the force superimposed on the rotating tool during the process or the tool sinking in the sheet have to be properly chosen. Finally both the rotating speed and the feed rate determine the heat flux during the welding process.

Quite a few investigations are found out in literature aimed to mechanically characterize the FSW with the focus to make nonlinear structural analysis [4]. It should be observed that the proper characterization of the material in the different zones of the joint is strictly needed in order to investigate the joint mechanical response and it would also allow to carry out effective numerical simulation of subsequent forming processes developed on the jointed blanks, i.e. bending or stamping of the so called tailored blanks [5].

The aim of the present paper is to investigate the tensile behaviour of a FSW butt joint through experiments and numerical simulations. For this purpose, beside the diffuse plastic strains produced by stress states exceeding the yield point, simulated by standard elastic-plastic finite elements, the localized damage and the subsequent formation of a macrocrack is reproduced by the presence of a cohesive elastic-damage interface model disposed along the weakest line of the welding. The obtained results permit to follow the plastic behaviour of the joint during the tensile test and also the fracture evolution of the joint.

2. EXPERIMENTAL INVESTIGATION

The considered joints were developed by FSW on AA6082-T6 3mm thick specimens, using properly designed clamping fixture to fix the specimens to be welded on a milling machine. As far as the utilized tool is regarded, it was made in H13 steel quenched at 1020 °C, characterized by a 52 HRc hardness; a cylindrical pin was used with the following geometrical characteristics: pin diameter equal to 4.00mm and pin height equal to 2.90mm; finally the shoulder diameter was equal to 10 mm. As the process parameters are regarded, a tool rotation speed of 1040 r.p.m., a tool feed rate of 100 mm/min, a tilt angle of 2° and a tool sinking of 2.9 mm were used on the basis of a previous experimental campaign developed by the authors [6].

The mechanical behaviour of the FSW joints and of the parent material was investigated through two series of tests, namely a standard uniaxial tension test and indenting tests carried out both in the unaltered metal and at points in the welding zones (TMAZ and HAZ).

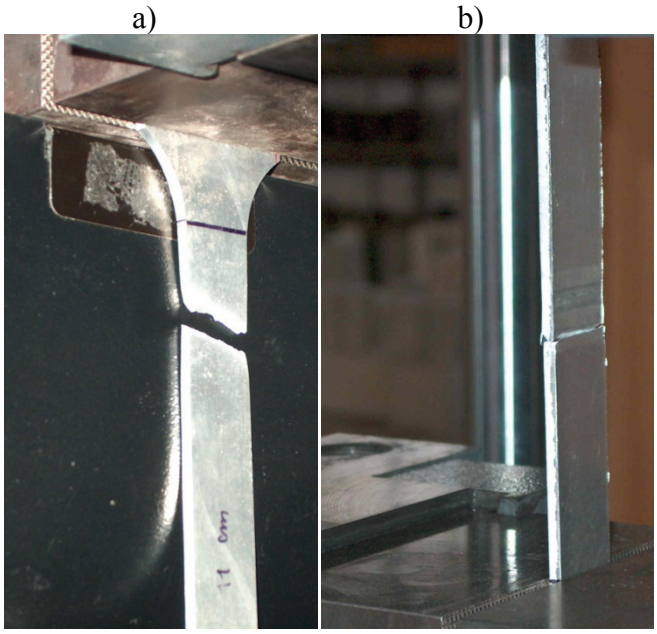

Fig. 1. *Tensile tests failure: a) plain continuous specimen; b) FSW specimen.*

Figure 1 shows the failure states obtained for the plain continuous metal sheet specimen (a) and the FSW one. It has been recognized that for the continuous one a typical shear band failure mode is produced, whereas for the welded specimen more complex phenomena are observed in the post elastic regime of the loading. Namely, for many tests, an initial strain localization shear band seems start to form (like the continuous specimen), but soon after a cohesive horizontal fracture along the weak welding line develops and propagate up to the complete separation fracture. The competition between the strain localization shear band, which seems to form first, and the subsequent dominant horizontal fracture (which produce an immediate unloading of the shear band) is a rather interesting aspect which deserve future studies and understanding.

In figure 2 the results in terms of engineering stress-strain curves of the tensile tests are shown for both the joints and the parent material. The presence of the FSW produce an overall decrement of the global strength of about 30%, together with a significant reduction of the ductility.

The indenting tests were developed through is a non-destructive technique for measurement of mechanical properties of materials. Further details on the technique can be found in [7-8]. In particular yield stress, ultimate tensile strength and strain hard-

ening exponent were obtained at 7 points in the transverse section of the welded joints at different distances from the welding line as shown in table 1, in which average values of experiment's results are reported (point 0 corresponds to the centre of welding line).

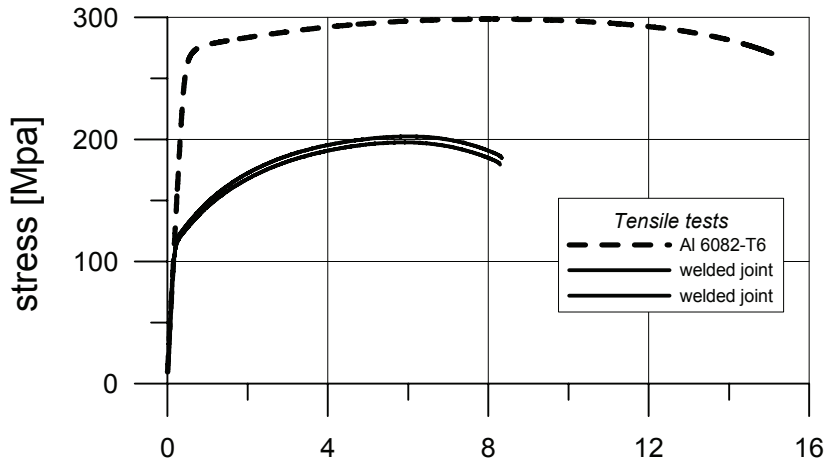

Fig. 2. *Stress-strain relation for uniaxial tension test.*

Table 1. *Numerical results related to the indentation test. Yield stress, ultimate stress and exponential hardening are evaluated at different distance from the welding center*

Distance [mm]	-12	-8	-4	0	4	8	12
σ_y [MPa]	225	159	160	164	161	156	228
σ_{TS} [MPA]	249	177	201	197	202	179	249
n	0,0959	0,0827	0,1331	0,1172	0,1324	0,089	0,091

It should be observed that the obtained results highlight the softening action determined by the FSW process on the material because of the generated heat flux; the strongest effect is not observed in the nugget at the core of the welding, due to dynamic recrystallization phenomena and consequent strongly reduced average grain size, which relatively improve the mechanical performances of the material [6], but in the TMAZ-HAZ zone where actually fractures occur during tensile tests.

3. FINITE ELEMENT SIMULATION

The finite element method has been adopted as an effective numerical tool capable to reproduce the detailed mechanical behaviour of structures with FSW lines [10]. The first attempt, which is useful to calibrate the model and the material constants, is the reproduction of the simple tension test. The structure has been discretized by 430 elastic-plastic finite elements (figure 3).

The constitutive relations adopted here are standard J2 associative plasticity law (von Mises) with linear isotropic strain hardening. The material constants (Elastic modulus, yield stress and hardening modulus) are spatially variable and they have been deducted by the local punch test described in the previous Section. In particular 7 zones have been considered. The elastic modulus E = 69 GPa and the linear isotropic hardening modulus H = 530 MPa has been selected equal at every point, whereas the yield stress σ_y varies in a piecewise constant form as shown in figure 4b). Figure 4 shows the measured value of the yield stress and the value adopted in the analysis.

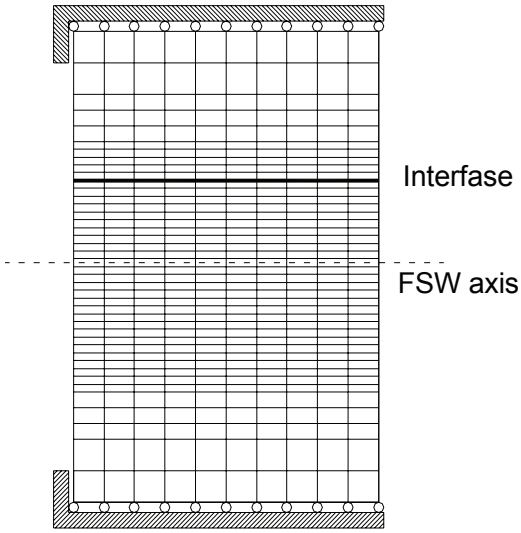

Fig. 3. *Finite Element mesh adopted for the analysis.*

As shown by the experimental results of figure 2, there is a load threshold after which strain softening appears. This softening regime is produced by localized damage which starts to be produced as microcracks in the weakest FSW zones. Microcracks increase porosity of the material and reduce the stiffness of the sound material as well as the load carry capacity. Usually this kind of behaviour is modelled by Gurson plasticity model, which anyway fails to predict a mesh objective solution as strain tends to localize along a line of fracture. An accepted solution is to modify the standard local plas-

ticity models by including strain gradient effects which ensure that the problem is well posed [11,12].

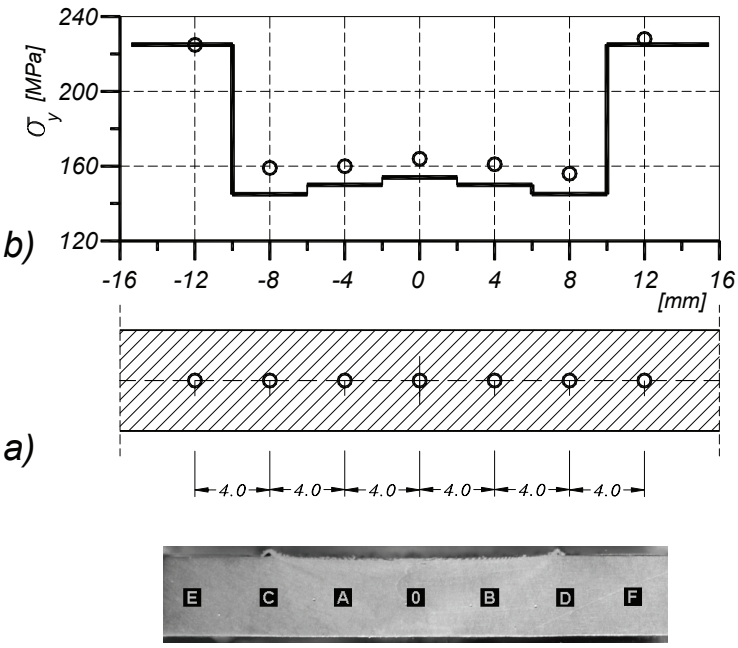

Fig. 4. *a) The indentation points. b) Yield stress vs, the distance from the welding centre (the dots are the experimental values and the solid line are the value assigned for the finite element analysis).*

Here, because of the specific welded problem, we adopt an interface element elastic-damage approach. Interface elements are disposed along the weakest line. They have zero thickness and describe in an average sense the elastic-damage properties which characterize the localized damage process zone. The introduction of the interface elements allow to follow the material response in the post peak softening regime, up to the complete failure, i.e. the full separation of the specimen in two pieces.

3.1. Interface model

The interface model adopted is a quite simple elastic-damage interface model. The state variable of the model are: displacement discontinuity jump vector [**u**], isotropic damage ω a scalar internal variable ξ, which represents the damage hardening evolution. The work conjugate variable are: the interface traction vector **t**, the energy release rate Y, and a static-like internal variable. The state equation which relate static to kinematics state variables are:

$$t_i = (1-\omega)K_{ij}[u_j] \tag{4a}$$

$$Y = \frac{1}{2}[u_i]K_{ij}[u_j] \tag{4b}$$

$$\chi = k\left[\ln\frac{c}{1-\xi}\right]^n \tag{4c}$$

where K_{ij} is a diagonal matrix collecting the interface elastic stiffness coefficients. The interface traction vector, for equilibrium reasons, has no discontinuity jump across the interface and it is related to the stress tensor at the adjacent bulk material by the Cauchy relation $t_i=\sigma_{ij}\ n_j$, where **n** is the outward normal at a point of the interface. Moreover, **t** represents the transfer strength capacity of the interface. In fact, eq. (4a) shows that for $\omega = 0$, which is the initial sound state, a complete stress transfer is ensured by the elasticity relation, whereas for $\omega = 1$, which means fully damaged state, no strength transfer is allowed.

Following a well established procedure, similar to the classical theory of plasticity, the damage activation function, together with the associative flow rules and with the damage loading/unloading condition, is defined as

$$\phi = Y - \chi \le 0 \tag{5}$$

$$\dot{\omega} = \frac{\partial\phi}{\partial Y}\dot{\lambda},\ \dot{\xi} = -\frac{\partial\phi}{\partial\chi}\dot{\lambda},\ \dot{\lambda} \ge 0,\ \phi\,\dot{\lambda} = 0. \tag{6}$$

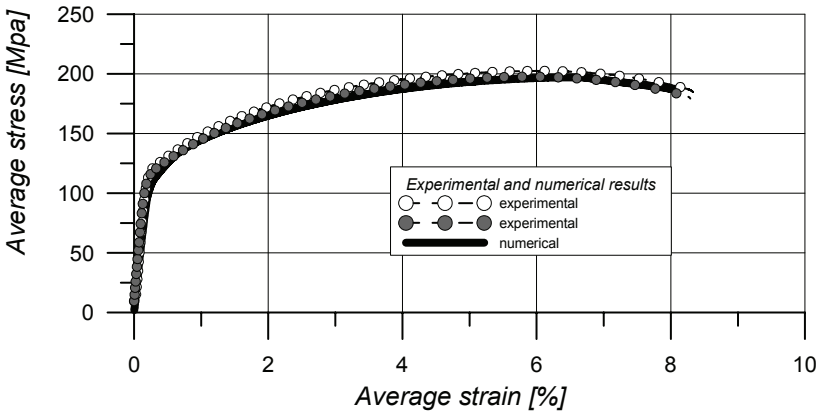

Fig. 5. *Average stress – average strain curve obtained by the finite element simulation compared with the experimental results.*

Equations (4), (5) and (6), which completely describe the interface damage constitutive equations, have been integrated stepwise in a fully implicit method and implemented in an interface finite ele-

ment. The date selected for the simulation are: $K_{11} = K_{22} = 50e5\,\mu\text{N}/\mu\text{m}^3$, $c = 3$, $n = 15.99$, $k = 12e\text{-}11$.

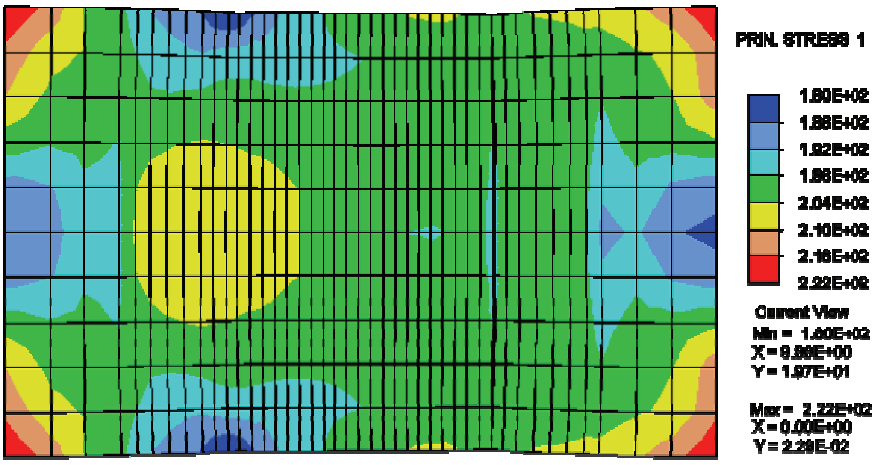

Fig. 6. *Map of maximum principal stress at the peak load level.*

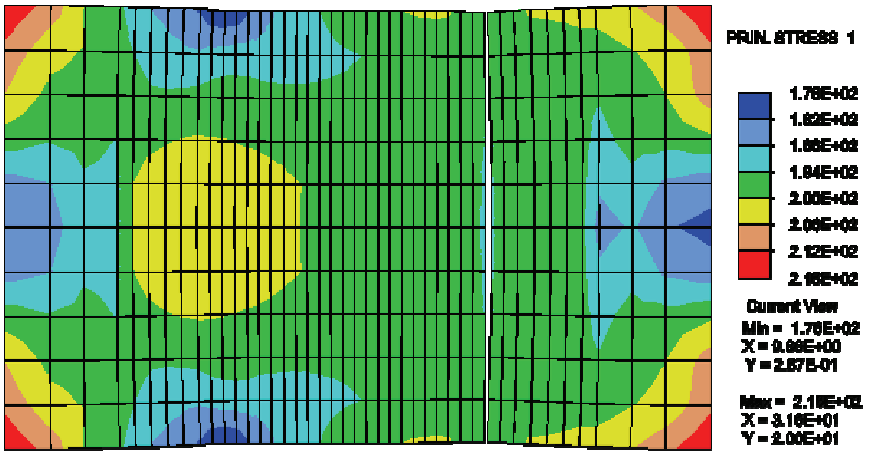

Fig. 7. *Map of maximum principal stress before collapse.*

3.2. Results

Figure 5 shows the average stress - average strain curves of the tension test compared with the analogous result obtained in the experimental test of figure 2. The average strain is obtained dividing the relative displacement by the initial measure length (L = 30 mm). Figure 5 shows the mesh adopted for the analysis.

Figure 6 shows the distribution of maximum principal stresses obtained by the numerical simulation at the highest load level. It can be observed that the damaging of the interface (displayed by a remarkable opening displacement at the central part of the interface) is already active before the descending branch of the average stress - average strain curves is reached. Figure 7 shows the principal stress distribution obtained by the numerical simulation, at the loading condition before the overall collapse in which a quite extended opening displacement is displayed.

4. DISCUSSION AND CONCLUSIONS

The friction stir welding technique was applied to joint Al6082-T6 and experimental tests were made. Two kinds of measurements were made, conventional tensile tests and local indentation tests to investigate mechanical properties of dissimilar zones of FSW welded joint.

The mechanical properties collected by tests were used to built a finite element model constituted by different plastic properties material zones, with inserted a zero thickness interface. The obtained numerical results were compared with tensile test ones, to verify correctness of the overall proposed model and showed a satisfying agreement.

It should be observed that the developed procedure neglects any variation of the material mechanical properties throughout the blank thickness, since the measurement points for the non-destructive measurement of mechanical properties of materials were taken just on the equatorial plane of the transverse section of the welded joints. The simulation, for instance, of bending mechanics based operations developed on the basis of the presented material characterization would then lead to poor results.

Anyway, the proposed approach seems promising in order to develop local material characterizations aimed to get necessary information in order to allow effective numerical analyses. In particular, with reference to FSW processes, on the basis of the quite complex material flow occurring during the welding, it is necessary to get a proper map of the material mechanical characteristics after welding covering all the different “material zones”. As further development of the present research the authors are going to take into account also the different material characteristics all along the sheet thickness

with the final aim to develop a complete procedure able to give indications and material data to be used in FEM simulations of sheet metal forming operations involving welded blanks.

ACKNOWLEDGEMENTS

This work has been made using MURST (Italian Ministry for University and Scientific Research) funds.

REFERENCES

1. Liu, H.J., Fujii, H., Maeda, M., Nogi, K., Tensile properties and fracture locations of friction-stir-welded joints of 2017-T351 aluminium alloy, J. of Mat. Proc. Tech., 142, 2003, 692–696.
2. Rhodes, C.G., Mahoney, M.W., Bingel, W.H., Spurling, R.A., Bampton, C.C., Effects of Friction Stir Welding on Microstructure of 7075 Aluminum, Scripta Materialia, 36, 1, 1997, 69-75.
3. Lee, W. B., Yeon, Y. M., Jung, S. B., The improvement of mechanical properties of friction-stir-welded A356 Al alloy, Mat. Science & Engineering, A355, 2003, 154-159.
4. Liu, S., Chao, Y.J., Determination of global mechanical response of friction stir welded plates using local constitutive properties, Modelling Simul. Mater. Sci. Eng., 13, 2005, 1-15.
5. Fratini, L., Buffa, G., Hua, J., Shivpuri, R., Friction Stir Welding of Tailored Blanks: Investigation on Process Feasibility, Annals of CIRP, 55/1, 2006, 279-282.
6. Barcellona, A., Buffa, G., Fratini, L., Process parameters analysis in friction stir welding of AA6082-T6 sheets, Proc. 7th ESAFORM Conference, ed., Storen, S., Trondheim, 2004, 371-374.
7. Ricciardi, R., Montanari, L.F., Moreschi, A., Sili, S., Storai, Mechanical characterisation of fusion materials by indentation test, Fusion Engineering and Design, 58-59, 2001, 755-759.
8. Scibetta, M., Lucon, E., Chaouadi, R., van Walle, E., Instrumented hardness testing using a flat punch, Int. J Pres. Ves. Piping, 80, 2003, 345-349.
9. Taljat, B., Zacharia, T., New analytical procedure to determine stress-strain curve from spherical indentation data, Int. J. Solids and Structures, 35, 1998, 4411-4426.
10. Zienkiewicz, O.C., The Finite Element Method, fourth ed., McGraw-Hill, UK,1991.
11. Polizzotto, C., Borino, G., A Thermodynamics-based forulation of gradient-dependendent plasticity, Eur. J. Mech. A/Solids, 17, 1998, 741-761.
12. Borino, G., Polizzotto, C., Thermodynamically consistent residual-based gradient plasticity theory and comparison, Modelling and Simulation in Material Science and Engineering, 15, 2007, 23-35.

MODELOWANIA PĘKANIA SPOIN OTRZYMANYCH Z PUNKTOWEGO ZGRZEWANIA TARCIOWEGO Z MIESZANIEM MATERIAŁU ZGRZEINY PODCZAS TESTU ROZCIĄGANIA

Streszczenie

Artykuł dotyczy mechanicznego modelowania i symulacji metodą elementów skończonych powstawania pęknięć w połączeniach spawanych aluminium uzyskanych metodą zgrzewania tarciowego z mieszaniem materiału zgrzeiny. Problem został przeanalizowany za pomocą modelu odkształceń skończonych, który określa przestrzenną propagację odkształceń plastycznych zapoczątkowaną w sąsiedztwie wydłużonych stref linii spawu. Ponadto, w symulacji uwzględniono model rozwarstwiania się materiału wzdłuż linii spawu.

Submitted: October 1, 2008
Submitted in a revised form: November 3, 2008
Accepted: November 3, 2008